OPEN

LKB1 Loss Induces Characteristic Patterns of Gene Expression in Human Tumors Associated with NRF2 Activation and Attenuation of PI3K-AKT

Jacob M. Kaufman, PhD, Joseph M. Amann, PhD,† Kyungho Park, BS,* Rajeswara Rao Arasada, PhD,† Haotian Li, BS,‡ Yu Shyr, PhD,§ and David P. Carbone, MD, PhD†*

Introduction: Inactivation of serine/threonine kinase 11 (*STK11 or LKB1*) is common in lung cancer, and understanding the pathways and phenotypes altered as a consequence will aid the development of targeted therapeutic strategies. Gene and protein expressions in a murine model of v-Ki-ras2 Kirsten rat sarcoma viral oncogene homolog (*Kras*)-mutant lung cancer have been studied to gain insight into the biology of these tumors. However, the molecular consequences of *LKB1* loss in human lung cancer have not been fully characterized.

Methods: We studied gene expression profiles associated with *LKB1* loss in resected lung adenocarcinomas, non–small-cell lung cancer cell lines, and murine tumors. The biological significance of dysregulated genes was interpreted using gene set enrichment and transcription factor analyses and also by integration with somatic mutations and proteomic data.

Results: Loss of *LKB1* is associated with consistent gene expression changes in resected human lung cancers and cell lines that differ substantially from the mouse model. Our analysis implicates novel biological features associated with *LKB1* loss, including altered mitochondrial metabolism, activation of the nuclear respiratory factor 2 (NRF2) transcription factor by kelch-like ECH-associated protein 1 (*KEAP1*) mutations, and attenuation of the phosphatidylinositiol 3-kinase and v-akt murine thymoma viral oncogene homolog (PI3K/AKT) pathway. Furthermore, we derived a 16-gene classifier that accurately predicts *LKB1* mutations and loss by nonmutational mechanisms. In vitro, transduction of *LKB1* into *LKB1*-mutant cell lines results in attenuation of this signature.

Conclusion: Loss of *LKB1* defines a subset of lung adenocarcinomas associated with characteristic molecular phenotypes and distinctive gene expression features. Studying these effects may improve our understanding of the biology of these tumors and lead to the identification of targeted treatment strategies.

Key Words: Genomics, LKB1, NRF2, PI3K/AKT.

(*J Thorac Oncol.* 2014;9: 794–804)

Departments of *Cancer Biology and §Biostatistics, Vanderbilt University, Nashville, Tennessee; †Department of Internal Medicine, James Thoracic Center, Ohio State University, Columbus, Ohio; and ‡University of Kentucky College of Dentistry, Lexington, Kentucky.

Disclosure: The authors declare no conflict of interest.

Address for correspondence: David P. Carbone, MD, PhD, James Cancer Center, The Ohio State University Medical Center, 488 Biomedical Research Tower, 460 West 12th Avenue, Columbus, OH 43210. E-mail: david.carbone@osumc.edu

ISSN: 1556-0864/14/0906-0794

Although genes activated by oncogenic mutations may be directly targetable with significant clinical benefit, strategies to target tumor suppressor loss depend on the identification and exploitation of differences in pathway activation or cellular phenotypes that occur as a consequence of these lesions. One such tumor suppressor is *LKB1*, a serine-threonine kinase tumor suppressor that is lost in approximately 30% of lung adenocarcinomas.[1,2] It is a key regulator of cellular metabolism through its control of the adenosine monophosphate–activated protein kinase (AMPK); loss of this metabolic checkpoint in tumors results in activation of the mammalian target of rapamycin (mTOR) pathway and susceptibility to metabolic stress.[3–5] LKB1 also affects development, cell polarity and motility, chromatin and transcriptional regulation, and cell growth by phosphorylating additional AMPK-family members and other mediators.[6,7] Understanding these complex interactions may help identify targeted strategies for treating *LKB1*-deficient tumors and determine feedback and resistance mechanisms that may differ between *LKB1*-wild-type and *LKB1*-mutant tumors.

To study these processes, genetically engineered murine models of *Lkb1/Kras*-mutant lung cancer have been developed. The resulting tumors are aggressive, metastasize readily, and exhibit diverse histological differentiation similar to that observed in human non–small-cell lung cancer (NSCLC).[1,8] This model implicates up-regulation of transforming growth factor-beta and v-src avian sarcoma (Schmidt-Ruppin A-2) viral oncogene homolog (SRC) pathways in the biology of these tumors and particularly in the progression to metastasis.[8] In vivo testing of treatment regimens demonstrates that these murine tumors exhibit sensitivity to metabolic stress induced by phenformin[5] but are resistant to mitogen activated protein kinase pathway inhibition.[9] Although mouse models are useful tools for studying tumor biology, the validity of the *Lkb1/Kras* lung tumor model in predicting human disease phenotypes has not been evaluated.

In this study, we describe gene expression changes and other molecular phenotypes associated with the loss of the *LKB1* tumor suppressor in human tumors and cell lines. Our approach is outlined in Figure 1. Loss of *LKB1* often occurs by somatic mutation,[7] but other mechanisms of inactivation also contribute, such as methylation, homozygous deletion, or intragenic deletions of one or more exons.[10–12] Inactivation of this tumor suppressor in lung cancer is thought to require

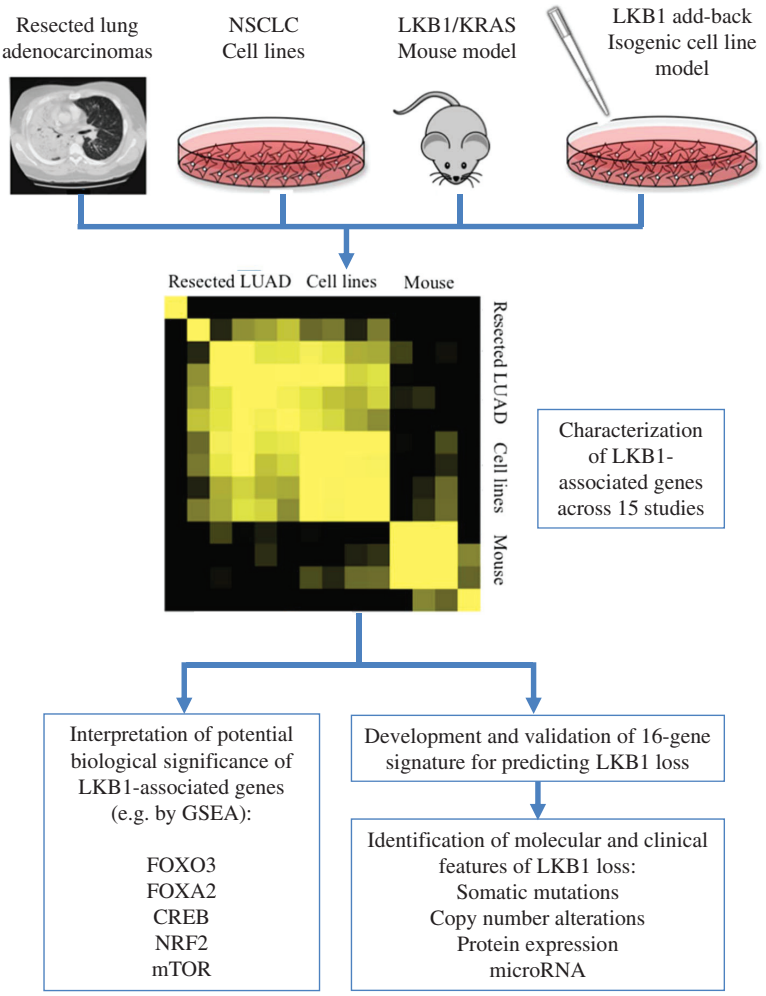

FIGURE 1. Schema showing analysis and experiments presented in this work. NSCLC, non–small-cell lung cancer; LKB1, liver kinase B1; KRAS, v-Ki-ras2 Kirsten rat sarcoma viral oncogene homolog; LUAD, lung adenocarcinoma; GSEA, gene set enrichment analysis; FOXO3, forkhead box O3; FOXA2, forkhead box A2; CREB, cAMP responsive element binding protein; NRF2, nuclear respiratory factor 2; mTOR, mammalian target of rapamycin.

complete or nearly complete loss of LKB1 function, regardless of the underlying mechanism. Thus, we will refer to these processes collectively as instances of "*LKB1* loss," or as an "*LKB1*-deficient" tumor, with the presumption—supported by our later findings—that these alterations yield similar tumor phenotypes.

Our analysis demonstrates that *LKB1* loss is associated with a consistent pattern of gene expression across resected human NSCLC tumors and cell lines. A predictive signature derived from this pattern accurately classifies mutational and nonmutational loss of *LKB1* in multiple validation sets. However, this pattern is not recapitulated in the murine model. Gene expression patterns and associations with other molecular features implicate activation of the forkhead box A2 (FOXA2), forkhead box O3 (FOXO3), cyclic-AMP responsive element binding protein (CREB), and NRF2 transcription factors and decreased PI3K/AKT signaling in tumors with *LKB1* loss. By defining these dysregulated processes, this work will guide future research efforts aimed at understanding the complex effects of these pathways in determining phenotypic and clinical consequences in tumors that have lost *LKB1*.

MATERIALS AND METHODS

Clinical and Molecular Data sets

Preprocessed and normalized data for RNAseq gene expression, microRNA expression, copy number alterations, protein expression, somatic mutations, and clinical data for lung adenocarcinomas characterized by The Cancer Genome Atlas (TCGA) were obtained from the TCGA Web site. Processed gene expression data, somatic mutations, and clinical information for other publicly available data sets were downloaded from Gene Expression Ominbus (GEO) and ArrayExpress or from individual Web sites, as listed in Supplementary Table S1 (Supplementary Digital Content 1, http://links.lww.com/JTO/A585). In cases where data were presented as linear expression values, log2 transformed values were used. The status of LKB1 loss in NSCLC cell lines was taken from various previous studies given in Supplementary Data File 1 (Supplementary Digital Content 2, http://links.lww.com/JTO/A586).

Gene expression analysis of A549 and H2122 cell lines transduced with pBABE, LKB1, or LKB1-K78I was performed using HT Human Gene 1.1 ST PM16 array plate

using a GeneTitan instrument (Affymetrix; Santa Clara, CA). They were then scanned on the Affymetrix Gene Titan AGCC v. 3.2.3 and then analyzed on Affymetrix Expression Console v. 1.1 using an robust multi-array average (RMA) normalization algorithm producing log2 results. These data are available from GEO data repository (GSE51266).

Statistical Analyses

Two-sided student's T-tests were used to compare statistical differences in continuous variable distributions between groups of samples: for instance, gene expression differences between *LKB1* wild-type and mutant tumors. For comparison of discrete variables such as the presence of somatic mutations, statistical significance was determined using Fisher's exact test. Statistical associations between continuous variables such as *LKB1* mRNA expression were determined using linear regression. Visualization of gene expression patterns by hierarchical clustering was performed with Cluster 3.0 and TreeView software packages. For the four expression clusters defined by hierarchical clustering, cluster "scores" were calculated for a given set of samples by averaging the standardized values of the respective genes. The score for the 16-gene *LKB1*-loss classifier, equivalent to the FOX/CREB cluster, was used for prediction of *LKB1* status in clinical and cell line samples. LKB1-loss scores for NSCLC cell lines are given in Supplementary Data File 1 (Supplementary Digital Content 2, http://links.lww.com/JTO/A586).

Gene expression associations for the four transcriptional clusters were calculated using multivariable general linear regression models carried out with the 'Limma' package in R bioconductor software, (R foundation for statistical computing, Vienna, Austria). Transcription factor analysis was performed using the Broad Institute's Molecular Signature Database,[13,14] and initial perturbation analysis was performed using the Connectivity Map.[15] Detailed information on data sources and statistical comparisons made for various analyses is given in Supplementary Table S1 (Supplementary Digital Content 1, http://links.lww.com/JTO/A585) and in Supplementary Methods (Supplementary Digital Content 3, http://links.lww.com/JTO/A587).

Cell Culture and Gene Transduction

A549 and H2122 cell lines were generously shared with us by John Minna and Luc Girard (University of Texas, Southwestern, Dallas, TX). Cell line identity was authenticated by DNA fingerprinting, and cell lines were tested to ensure that they were mycoplasma negative. Cells were cultured in Roswell Park Memorial Institute 1640 (RPMI1640) cell growth media, (GIBCO, Carlsbad, CA) containing 5% fetal bovine serum, without antibiotics. Empty pBABE viral plasmids, pBABE-LKB1 and pBABE-LKB1-K78I, were obtained from Addgene (Cambridge, MA). Phoenix cells were transfected with viral plasmids and retroviral particles were harvested from media supernatant 48 hours after transfection. Viruses were added to target cells with polybrene, and selection with 1 μg/ml puromycin was begun 48 to 72 hours after infection. Cells were selected under puromycin for 1 to 2 weeks before performing subsequent experiments, with experiments being completed within 2 months.

Immunoblots

Cell lysates were harvested while cells were in exponential growth phase in radioimmunoprecipitation assay (RIPA) lysis buffer containing phosphatase and protease inhibitors. Lysates were homogenized and run on precast sodium dodecyl sulfate–polyacrylamide gel electrophoresis gels (BioRad, Hercules, CA). Phospho-ACC (s79), ACC, RS6, and LKB1 antibodies were obtained from Cell Signaling Technology, Danvers, MA.

CRE-Luciferase Reporter

We designed a dual-luciferase reporter driven by a ×3 cyclic-AMP responsive element (CRE) consensus-binding sequence in the promoter region in addition to a TATA box, which was inserted into a lentiviral construct upstream of luciferase. Luciferase activity from this reporter was compared with a control reporter that was identical but with mutated CRE sites. Cells were stably transduced to express CRE-wild-type or CRE-mutant reporters and ratios between the two were compared after subsequent perturbations.

More detailed descriptions of statistical and analytical procedures are available with Supplementary Methods online (Supplementary Digital Content 3, http://links.lww.com/JTO/A587).

RESULTS

LKB1 Loss Results in Consistent Gene Expression Changes in Human Tumors

The effects of signaling pathways are mediated in part by activation of transcription factors affecting the expression of downstream genes. Inferences drawn from the analysis of the dysregulated genes may disclose novel links between pathways and phenotypes that would otherwise be difficult to predict. We determined gene expression changes associated with *LKB1* loss in lung adenocarcinomas characterized by the TCGA (Cancer Genome Atlas Research Network). Comprehensive molecular characterization of lung adenocarcinoma. *Nature*. 2014), as well as five additional studies of resected lung adenocarcinomas[16–20] two large collections of NSCLC cell lines[21,22] and data from two studies using the *Lkb1/Kras* murine model[1,8] (Supplementary Table S1, Supplementary Digital Content 1, http://links.lww.com/JTO/A585). Genes with differential expression between *LKB1*-mutant and *LKB1*-wild-type samples were ranked by statistical significance for each data set (Supplementary Data File 2, Supplementary Digital Content 4, http://links.lww.com/JTO/A588). These *LKB1*-associated gene lists were then compared pairwise across all data sets, and statistical significance of overlapping genes was used to determine similarity (Fig. 2*A*; Supplementary Figure S1 [Supplementary Digital Content 5, http://links.lww.com/JTO/A589]; Supplementary Table S2 [Supplementary Digital Content 1, http://links.lww.com/JTO/A585]). A consistent pattern of gene expression is associated with *LKB1* loss across human data sets (median *p* value = 3.8e-18 for 55 pairwise comparisons). Murine *Lkb1* loss also resulted in a consistent gene expression signature across the two studies, but without significant overlap with the human studies, suggesting important differences in tumor

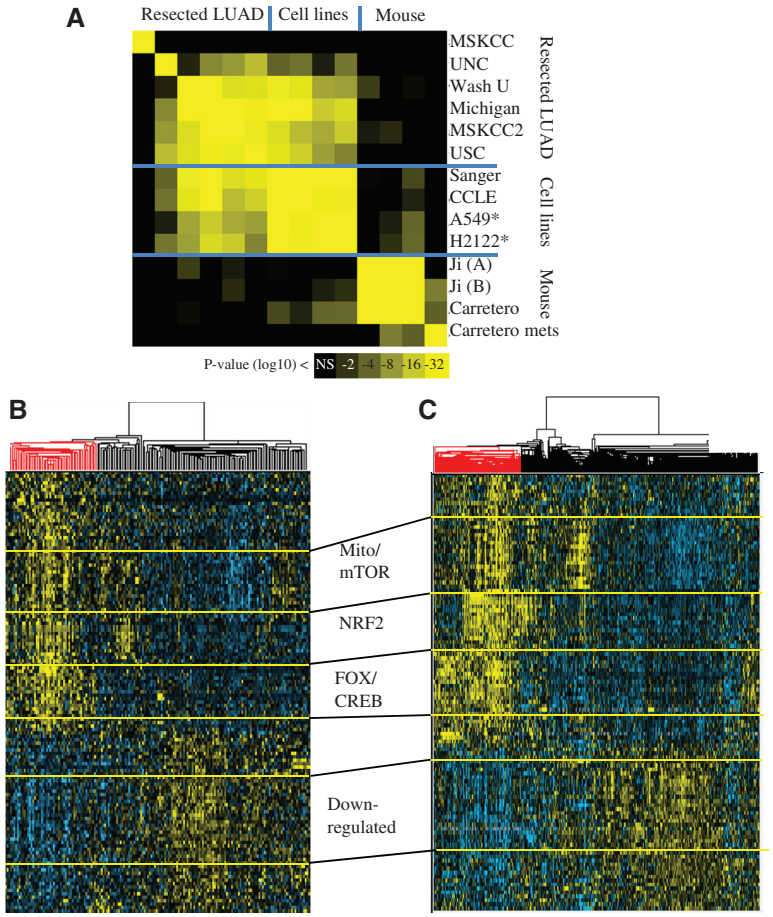

FIGURE 2. *LKB1* loss produces a characteristic pattern of gene expression. *A,* The statistical significance of gene overlap is shown for pairwise comparisons of the top 200 genes overexpressed in tumors with *LKB1* loss in 15 studies of lung adenocarcinomas. Asterisks indicate comparisons between cell lines expressing vector control and those expressing wild-type *LKB1*. The two cell line studies, CCLE and Sanger, contain many overlapping cell lines; thus, their results were not independent but demonstrate consistency of these patterns across the two data sets. *p* values from a hypergeometric test are color coded according to the legend. *B* and *C,* Unsupervised hierarchical clustering of resected lung adenocarcinomas from the (*B*), Michigan cohort from the Director's Challenge study ($n = 178$) or (*C*) from the TCGA ($n = 446$) using a 129 gene signature of *LKB1* loss. Tumors are shown on the horizontal axis, with loss of *LKB1* highlighted in red; genes are represented on the vertical axis. Four clusters of genes, demarcated by yellow lines, are observed in each of these data sets. TCGA, The Cancer Genome Atlas; LUAD, lung adenocarcinoma; MSKCC, Memorial Sloan Kettering Cancer Center; UNC, University of North Carolina; CCLE, Cancer Cell Line Encyclopedia; NS, not significant; LKB1, liver kinase B1; mTOR, mammalian target of rapamycin; NRF2, nuclear respiratory factor 2; FOX, forkhead box; CREB, cyclic-AMP responsive element binding protein.

biology (Fig. 2*A*; Supplementary Figure S1 [Supplementary Digital Content 5, http://links.lww.com/JTO/A589]).

Having established that *LKB1* loss results in consistent patterns of gene expression in human lung adenocarcinomas, we used two clinical data sets—one analysis of lung adenocarcinomas from University of Michigan ($n = 178$) and one characterized by Washington University ($n = 41$)—as training cohorts to identify 129 genes associated with *LKB1* loss (Supplementary Data File 2, Supplementary Digital Content 4, http://links.lww.com/JTO/A588). Expression of these genes was visualized using hierarchical clustering, as shown for the Michigan training set and the TCGA validation set (Fig. 2*B, C*). Comparison of the correlation patterns in these two data sets allows identification of four consistently expressed transcriptional clusters (Fig. 2*B, C*; Supplementary Figure S2 [Supplementary Digital Content 5, http://links.lww.com/JTO/A589]). However, the correlation patterns of the down-regulated genes were not as reproducible across multiple data sets as the up-regulated genes, so we will focus our attention on the three clusters that show increased expression in *LKB1*-deficient tumors.

Computational Approaches Identify Putative Drivers of Expression Clusters Associated with LKB1 Loss

The pattern of gene expression associated with *LKB1* loss may be reflective of biological processes altered in these tumors. We sought to identify transcription factors putatively associated with these genes using a bioinformatics approach. For each of the four clusters identified, ranked lists of gene expression association were determined using a multivariable linear model. The top 200 genes associated with each cluster were then used to generate hypotheses regarding the pathways or phenotypes that drive the expression of these clusters by mining public data sources, including predicted promoter transcription factor–binding sites,[13] drug-induced perturbations characterized by the connectivity map project,[15] and the diverse collections of predetermined genesets included in the molecular signature database.[13,14]

Two of the up-regulated clusters showed associations with tumor metabolic phenotypes. The "mTOR/mitochondria" cluster was associated with high expression of oxidative phosphorylation and mitochondria-associated genes and genes involved in protein translation (Supplementary Table S3, Supplementary Digital Content 1, http://links.lww.com/JTO/A585). The "NRF2" cluster contains oxidative stress response genes driven by the NRF2 transcription factor (Supplementary Table S4, Supplementary Digital Content 1, http://links.lww.com/JTO/A585). As LKB1 functions in conjunction with AMPK as a metabolic regulator,[6,7,23] these phenotypes may either represent direct metabolic consequences of *LKB1* loss or adaptive responses to compensate for loss of protective mechanisms.

Analysis of a third cluster of up-regulated genes implicated CREB, FOXO, and FOXA2 transcription factors (Supplementary Table S5, Supplementary Digital Content 1, http://links.lww.com/JTO/A585). Of the four gene clusters identified, the FOX/CREB cluster had the strongest association with LKB1 loss in the training cohort. Analysis of perturbed genes from the connectivity map also revealed induction of this cluster by colforsin, an adenylate cyclase stimulator that activates CREB, and by the typical antipsychotics thioridazine, prochlorperazine, and trifluoperazine, which have been identified as stimulators of FOXO transcription factors.[24] We then searched the GEO and Array Express data repositories and found corroborating evidence for CREB and FOXO3 activation within this cluster. Furthermore, analysis of chromatin precipitation data[25] showed significantly increased levels of *FOXA2* promoter occupancy among these genes in A549 and HEPG2 cells. Thus, this cluster may represent the effects of a specific set of transcription factors that are dysregulated downstream of LKB1.

Wild-Type LKB1 Attenuates the LKB1-Associated Signature

To test whether LKB1 could exert direct effects on gene expression, we used an isogenic cell line model system in which LKB1 was stably expressed in LKB1-mutant NSCLC cell lines (A549 and H2122). Mutated LKB1-K78I and empty pBABE retrovirus were used as controls. LKB1 expression was confirmed by Western blot, and kinase activity was shown

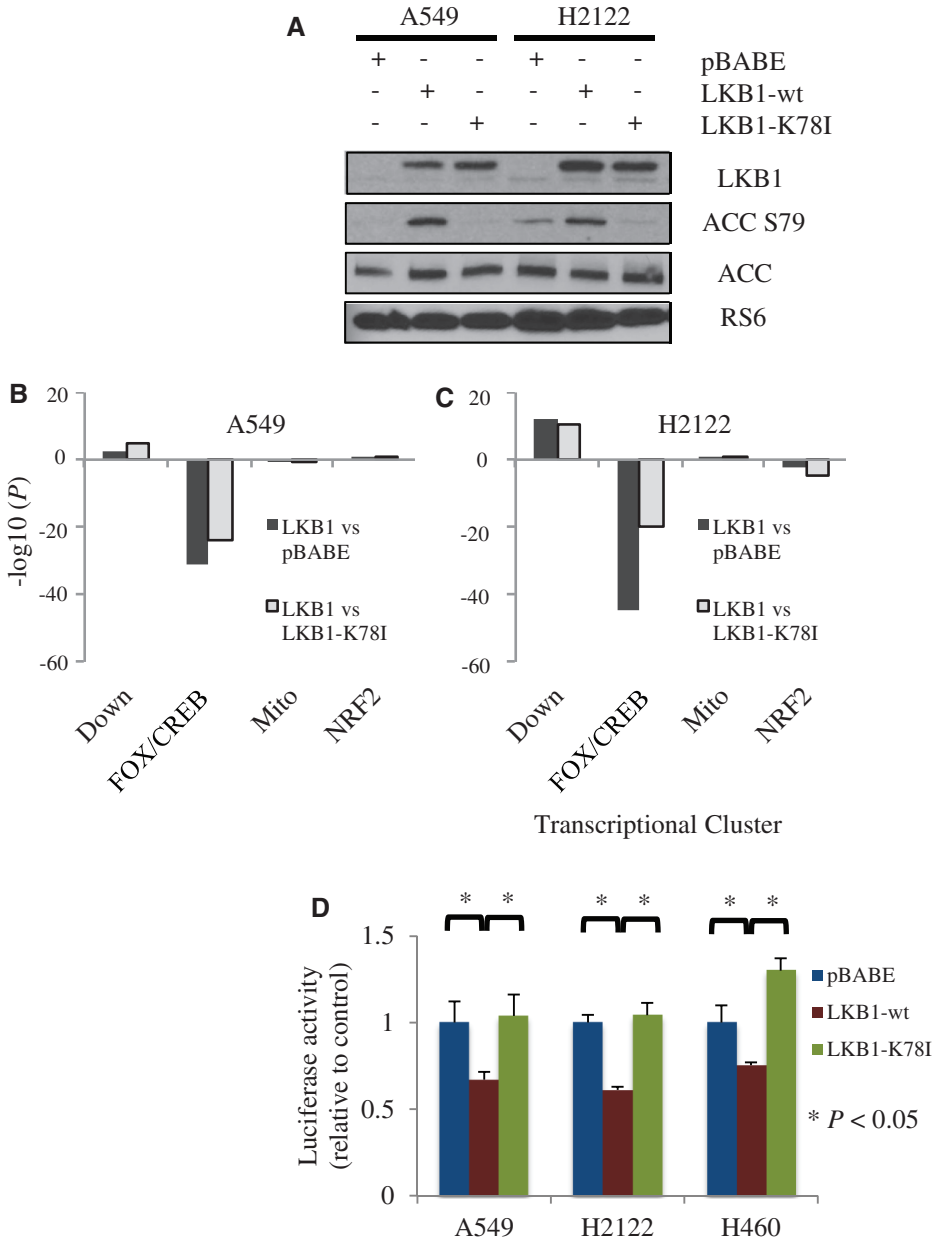

FIGURE 3. Restoring wild-type LKB1 attenuates the expression of the LKB1-deficient gene signature and the CREB transcription factor. *A,* Immunoblots of whole-cell lysates from A549 and H2122 stably expressing empty pBABE vector, LKB1 or K78I LKB1. Ribosomal protein S6 is used as a loading control. *B* and *C,* Changes in gene expression of A549 (*B*) or H2122 (*C*) cell lines after re-expressing wild-type or mutant *LKB1* were compared with the gene lists for each of the four *LKB1*-associated clusters using a hypergeometric test. Log10 *p* values are indicated on the *y* axis, with positive values indicating induction of expression and negative values indicating repression. *D,* Activity of CRE-luciferase is shown for A549 and H2122 cell lines after stable expression of LKB1 or K78I LKB1. Reporter activations were determined relative to a control luciferase with mutated CRE sites and are shown relative to the pBABE control. *p* values show the significance of unpaired student's *t* tests. LKB1, liver kinase B1; CREB, cyclic-AMP responsive element binding protein; pBABE, pBABE retrovirus; FOX, forkhead box protein; NRF2, nuclear respiratory factor 2.

by demonstrating that wild-type LKB1 resulted in phosphorylation of acetyl-CoA-carboxylase, a downstream target of AMPK (Fig. 3*A*) in A549 and H2122 cells.

Global gene expression analysis showed that genes directly altered by LKB1 expression in A549 and H2122 showed significant overlap with the differentially expressed genes from our analysis of clinical and cell line data sets (Fig. 2*A*; Supplementary Figure 1 [Supplementary Digital Content 5, http://links.lww.com/JTO/A589]). By comparing the overlap of LKB1-perturbed genes to each of the top 200 genes associated with the four gene clusters from our previous analysis, we show that genes affected directly by LKB1 expression showed the strongest association with the FOX/CREB gene cluster (hypergeometric test p values = 1.3e-30, 3.6e-45 for A549 and H2122; Fig. 3*B, C*), whereas mTOR/mitochondria and NRF2-associated clusters were relatively unaffected. Many of the 16 individual genes that originally identified the FOX/CREB cluster were down-regulated by twofold or more in response to LKB1 expression (Supplementary Figure S3, Supplementary Digital Content 5, http://links.lww.com/JTO/A589). Because this gene cluster was linked in part to CREB activity, we also tested CREB transcriptional activity in A549 and H2122 cell lines using a luciferase reporter driven by the CREB-consensus sequence, which showed a reduction in reporter activity of 30% to 40% (Fig. 3*D*; $p < 0.05$ for each cell line). This is consistent with previous studies showing CREB to be directly attenuated downstream of LKB1 due to effects on the CREB regulated transcription coactivator (CRTC) family of transcriptional coactivators.[26–28]

A 16-Gene Classifier Accurately Predicts LKB1 Mutations in Lung Adenocarcinoma

The FOX/CREB cluster showed a strong association with LKB1 mutations in the training cohort and its expression was also directly attenuated by the restoration of wild-type LKB1 in vitro. Thus, we tested the ability of a 16-gene classifier (*AVPI1, BAG1, CPS1, DUSP4, FGA, GLCE, HAL,*

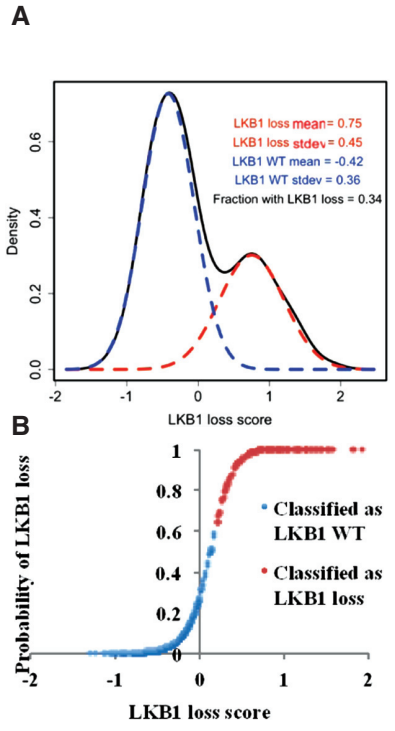

C

Dataset	LKB1 status (n)	Sensitivity (%)	Specificity (%)	P-value
Pooled	Mut: 26 WT: 213	85	76	2.8e-09
TCGA	Mut: 67 WT: 339	97	78	2.5e-33
Cell lines	Mut: 39 WT: 46	93	91	1.2e-16

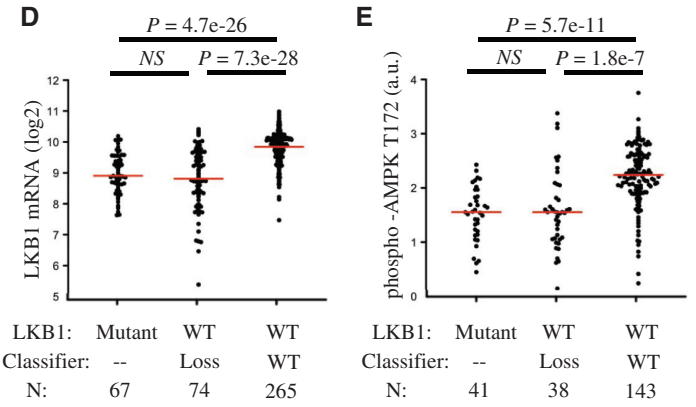

FIGURE 4. A 16-gene signature of *LKB1* loss accurately predicts *LKB1* mutations, loss of LKB1 expression, and loss of function. *A*, The population distribution is shown for numeric *LKB1*-loss scores calculated for 446 lung adenocarcinomas from the TCGA. Parameters are shown for calculations of best fit to a bimodal distribution; these parameters, and the two associated normal distributions, are shown. *B*, On the basis of the parameters for the two normal distributions determined for this population, the probability of a given score representing the high-expression *LKB1* loss curve is shown. *C*, Sensitivity and specificity of the *LKB1* classifier for prediction of *LKB1* mutations across independent testing sets; *p* value represents the result of the Fisher's exact test. *D*, Expression of *LKB1* mRNA is shown for TCGA lung adenocarcinomas grouped by *LKB1* mutation and *LKB1*-loss signature classification status. *E*, Expression of phospho-AMPK T172 is shown for the subset of TCGA lung adenocarcinomas with RPPA data, which were grouped by *LKB1* mutation and *LKB1*-loss signature classification status. *D* and *E*, Each dot represents one tumor, with red bars indicating the median expression. *p* values represent results from the student's *t* test comparing indicated groups. RPPA, reverse phase protein array; TCGA, The Cancer Genome Atlas; AMPK, adenosine monophosphate–activated protein kinase; LKB1, liver kinase B1; WT, wild-type; NS, not significant.

IRS2, MUC5AC, PDE4D, PTP4A1, RFK, SIK1, TACC2, TESC, and *TFF1*) representing this gene cluster to discriminate *LKB1*-deficient tumors from those with functional *LKB1*. Standardized gene values were averaged for these 16 genes to give a single numeric score for each tumor in a data set. These scores exhibited a bimodal distribution, from which we could estimate a class probability and calculate an inherent misclassification rate of 6.5% because of the region of overlap in the two underlying distributions (Fig. 4*A*, *B*). A cutoff value of 0.2 was selected from the training analysis and was used to classify tumors as *LKB1* wild-type or *LKB1* loss.

We then tested the ability of the signature to predict *LKB1* mutations in independent validation sets: a pooled analysis of previously published resected lung adenocarcinomas, lung adenocarcinomas characterized by TCGA (Cancer Genome Atlas Research Network. Comprehensive molecular characterization of lung adenocarcinoma. *Nature.* 2014), and NSCLC cell lines. No samples from these validation sets were used at any point in the derivation of our signature from the stated training sets. *LKB1* mutations were accurately predicted in each of the lung cancer validation cohorts with a combined sensitivity of 93%; 22 of 26 somatic *LKB1* mutations in the pooled cohort, 65 of 67 in the TCGA cohort, and 36 of 39 in NSCLC cell lines (sensitivity 85%, 97%, and 92%; p = 2.8e-9, 2.5e-33, and 1.2e-16; shown in Fig. 4*C* and Supplementary Figure S4, Supplementary Digital Content 5, http://links.lww.com/JTO/A589).

We further tested our *LKB1*-loss signature alongside previously reported studies by using gene set enrichment analysis to compare the various gene lists to the genes differentially expressed by LKB1 mutant tumors in the largest dataset - the TCGA cohort - and those directly perturbed by *LKB1* in our in vitro study. The previous work available for comparison include three studies that examined the in vitro effects of LKB1 add-back in A549,[1,29] H2126,[1] and HeLa[30] cells, a previous report of gene expression changes associated with *LKB1* mutations,[31] and expression profiles associated with the "magnoid" subtype of lung adenocarcinomas,[18] which has been shown to have an increased prevalence of *LKB1* mutations (Supplementary Table S6, Supplementary Digital Content 1, http://links.lww.com/JTO/A585). This analysis shows that *LKB1* has consistent effects on gene expression in cell lines seen in our analysis and previous work, including similar changes in the nonlung HeLa cell line. The genes identified by Fernandez et al. do not seem to be reproducibly associated with *LKB1* loss in our analysis. On the other hand, genes associated with the "magnoid" subtype show significant overlap with *LKB1*-associated genes, but to a much lesser extent than is observed for the *LKB1*-loss signature.

LKB1 Wild-Type Lung Adenocarcinomas That Express the *LKB1*-Loss Signature Show Evidence of *LKB1* Inactivation

Twenty-three percent of tumors without known *LKB1* mutations were classified as having *LKB1* loss. However, some mutations may have been unrecognized, and there are multiple mechanisms by which tumor suppressors can be inactivated in addition to somatic mutation.[10–12] Thus, we looked for additional evidence of *LKB1* loss by examining *LKB1* mRNA expression measured by RNAseq, and LKB1 protein expression and phosphorylation of AMPK-T172 in the subset of tumors that were also characterized by reverse phase protein array. Among the 67 tumors with identified mutations in *LKB1*, *LKB1* mRNA expression and phospho-AMPK are strongly decreased (Fig. 4*D, E*; p = 4.7e-26 and 5.7e-11, respectively, by Student's t test). Low pAMPK is consistent with the loss of LKB1 kinase activity, whereas decreased mRNA expression reflects the fact that of these 67 mutations, 49 (73%) are nonsense, splice site, or frameshift alterations that are expected to lead to reduced mRNA expression by nonsense-mediated decay.[32] LKB1 protein is also decreased among these 67 mutant tumors (p = 0.030); the moderate statistical significance associated with this observation compared with that associated with phosphorylated AMPK may reflect differences in antibody specificity.

When the same analysis is applied to the 74 *LKB1* wild-type tumors that express the *LKB1*-loss gene signature, these tumors exhibit the same characteristics of *LKB1* loss: these tumors have low *LKB1* mRNA expression (p = 7.3e-28; Fig. 4*D*), low LKB1 protein expression (p = 0.011), and show loss of LKB1 kinase activity as demonstrated by attenuated phosphorylation of AMPK-T172 (p = 1.7e-7; Fig. 4*E*). Moreover, when the 67 tumors with known *LKB1* mutations are compared with the 74 *LKB1*-wild-type tumors that are predicted to have *LKB1* loss, no significant differences are observed in LKB1 protein or mRNA expression or of AMPK phosphorylation (Fig. 4*D, E*). These tumors likely represent unrecognized cases of *LKB1* loss that could occur by undetected mutation, intragenic deletion, chromosomal loss, or by an epigenetic mechanism. This finding suggests that the classifier may significantly surpass the observed specificity of 77% and shows that the *LKB1*-loss classifier is more sensitive than DNA sequencing for the detection of functional *LKB1* loss.

Determination of Other Tumor Characteristics Associated with LKB1 Loss

Differentially expressed genes associated with *LKB1* loss can be studied directly to infer patterns of transcription factor activation that may reflect underlying differences in pathway activation. To better understand other phenotypes of *LKB1* loss, we performed statistical comparisons to determine differences in clinical characteristics, copy number alterations, microRNA expression, protein expression, and mutation prevalence between *LKB1*-wild-type lung adenocarcinomas and those with *LKB1* loss (Fig. 5, Supplementary Tables S7–S10, Supplementary Digital Content 1, http://links.lww.com/JTO/A585). The 16-gene classifier was used to determine *LKB1* status of TCGA-characterized lung adenocarcinomas for the purpose of these comparisons.

To uncover novel associations between *LKB1* loss and alterations in other pathways, we studied the prevalence of somatic mutations in the TCGA cohort of lung adenocarcinomas using a defined set of cancer genes (Catalog of Somatic Mutations in Cancer [COSMIC] Cancer Gene Census). Of the 32 genes with at least a 5% mutation rate in this cohort, five

A

	Association with LKB1 loss			Fisher's exact test		
	Number of Samples		Fraction with LKB1 loss (%)	Odds Ratio (95% C.I.)	P-value	Q-value
	Total	LKB1 loss				
KEAP1 mutant	71	50	70.4	6.8 (3.7, 12.6)	3.2E-12	6.30E-10
KEAP1 wild-type	332	86	25.9			
EGFR mutant	58	2	3.4	0.056 (0.0066, 0.22)	5.9E-09	6.3E-08
EGFR wild-type	345	134	38.8			
TP53 mutant	212	46	21.7	0.31 (0.20, 0.49)	1.04E-07	8.3E-07
TP53 wild-type	191	90	47.1			
KRAS mutant	117	57	48.7	2.5 (1.6, 4.0)	7.3E-05	0.00047
KRAS wild-type	286	79	27.6			
ATM mutant	36	22	61.1	3.5 (1.6, 7.6)	6.5E-04	0.0035
ATM wild-type	367	114	31.1			

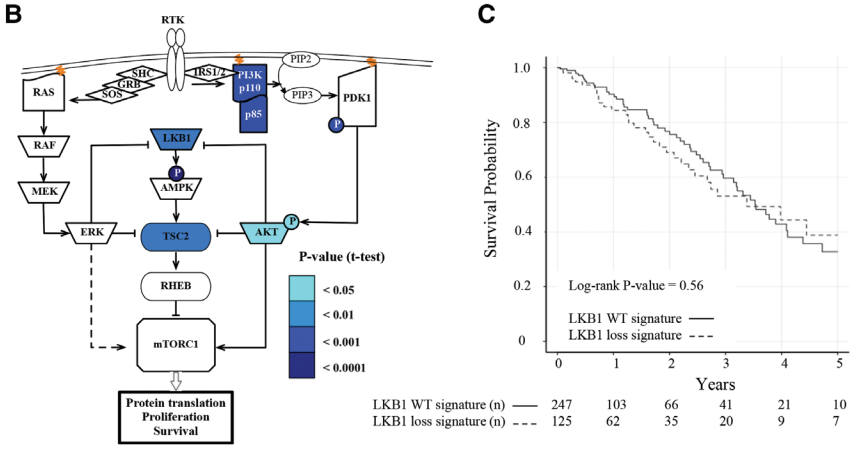

FIGURE 5. Clinical and molecular features associated with *LKB1* loss. *A*, Somatic mutations in key cancer genes occur at different frequencies among tumors with *LKB1* loss. Fisher's exact test was used to compare mutation count data from exome sequencing data among lung adenocarcinomas characterized by the TCGA and classified using the *LKB1*-loss signature as either *LKB1* wild-type ($n = 267$) or *LKB1*-loss ($n = 136$). Analysis was limited to genes with a mutation prevalence of at least 5% taken from a specified list of cancer-related genes ($n = 32$). Q-values represent correction of raw p values for this multiple hypothesis testing. *B*, Schema showing the role of the PI3K/AKT pathway in regulating mTOR activity. Analysis of differential protein or phosphorylation expression was performed with the Student's t test, using RPPA data from lung adenocarcinomas characterized by the TCGA and classified using the *LKB1*-loss signature as either *LKB1* wild-type or *LKB1*-loss. Selected proteins are shown using colors that correspond to p values indicated in the legend, with blue indicating decreased expression in tumors with *LKB1* loss. The complete list of differentially expressed proteins is given in Supplementary Table S9 (Supplementary Digital Content 1, http://links.lww.com/JTO/A585). *C*, Resected lung adenocarcinomas characterized by TCGA ($n = 372$) were classified as *LKB1*-loss or *LKB1* WT using the *LKB1*-classifier score. Kaplan–Meier curves were used to plot cumulative events for these two groups for overall survival, p value represent the results of the log-rank test; the number of evaluable tumors remaining are given at yearly intervals below the plot. RPPA, reverse phase protein array; TCGA, The Cancer Genome Atlas; CI, confidence interval; AMPK, adenosine monophosphate–activated protein kinase; LKB1, liver kinase B1; KEAP1, kelch-like ECH-associated protein 1; EGFR, epidermal growth factor receptor; KRAS, v-Ki-ras2 Kirsten rat sarcoma viral oncogene homolog; ATM, ataxia telangectasia mutated; PI3K, phosphatidylinositiol 3-kinase; PIP2, phosphatidylinositol 4,5-bisphosphate; RAS, rat sarcoma (RAS) oncogene family; RAF, v-Raf oncogene family; MEK, MAPK/ERK kinase; ERK, extracellular regulated signal kinase; RHEB, Ras homolog enriched in brain; SOS, son of sevenless; GRB, growth factor receptor-bound protein ; SHC, Src homology 2 domain containing transforming protein; IRS, insulin receptor substrate; PDK1, 3-phosphoinositide-dependent protein kinase 1; TSC2, tuberous sclerosis complex 2; mTOR, mammalian target of rapamycin; WT, wild-type; AKT, v-akt murine thymoma viral oncogene homolog.

showed significant differences on the basis of *LKB1* status. *KRAS*, *KEAP1*, and *ATM* were mutated more frequently in tumors that had lost *LKB1*, whereas *EGFR* and *p53* mutations were less common (Fig. 5*A*). We were able to test associations with *EGFR*, *KRAS*, and *p53* mutations independently using a pooled analysis of publicly available lung adenocarcinoma cohorts. Consistent with results from a prior study,[33] this analysis confirmed fewer *EGFR* mutations ($p = 1.9e\text{-}10$) and increased prevalence of *KRAS* mutations ($p = 0.00035$) among tumors with *LKB1* loss. No association with p53 loss was

observed in this pooled analysis, so this finding is of uncertain significance. No data set was available to directly confirm associations with *ATM* and *KEAP1* mutations. However, tumors with *KEAP1* loss exhibited high levels of the "NRF2 cluster" of gene expression, consistent with the direct role of KEAP1 in the degradation of the NRF2 transcription factor (Supplementary Figure S5, Supplementary Digital Content 5, http://links.lww.com/JTO/A589). Thus, expression of this cluster seems to be indirectly linked to *LKB1* loss, reflecting instead the increased prevalence of *KEAP1* loss in these tumors.

Associations between *LKB1* loss and copy number alterations (Supplementary Table S7, Supplementary Digital Content 1, http://links.lww.com/JTO/A585), microRNA expression (Supplementary Table S8, Supplementary Digital Content 1, http://links.lww.com/JTO/A585), and protein expression (Supplementary Table S9, Supplementary Digital Content 1, http://links.lww.com/JTO/A585) were also determined using TCGA data. Findings from analysis of reverse phase protein array proteomic data may be of particular interest, because these can potentially reflect states of pathway activation that may be important for developing targeted interventions for *LKB1*-deficient tumors. Expression levels for 186 proteins and phosphorylated protein sites were compared between these groups using the Student's *t* test. Several components of the PI3-kinase pathway were down-regulated among tumors with *LKB1* loss, suggesting that this pathway may be attenuated in these tumors. Differentially expressed proteins and phosphorylations are mapped onto a schematic drawing representing key features of this pathway[34–36] (Fig. 5*B*). Both the p85 and p110 subunits of PI3K showed significant decrease in expression ($p = 0.00061$ and 0.00047, respectively), as well as decreased phosphorylation of PDK1 at serine 241 ($p = 0.00012$), and decreased total Akt ($p = 0.02$) and phospho-S473 Akt ($p = 0.018$). Surprisingly, proteomic evidence did not suggest significant mTOR activation, showing only modest increase in eIF4E expression and decrease in 4E-BP1 ($p = 0.037$ and 0.032, respectively), with no significant differences in other components of mTOR signaling. A complete list of the significant associations seen in this analysis is given in Supplementary Table S9 (Supplementary Digital Content 1, http://links.lww.com/JTO/A585).

Finally, we show that *LKB1* loss has no prognostic significance in lung adenocarcinoma (Fig. 5*C*). There is no association with tumor stage or survival in either the TCGA or Director's Challenge cohorts (Supplementary Table S10, Supplementary Digital Content 1, http://links.lww.com/JTO/A585). Smoking status was the only clinical characteristic associated with *LKB1* loss, with tumors arising from never-smokers exhibiting a significantly lower prevalence of *LKB1* loss. These findings are consistent with prior analysis of the clinical significance of *LKB1* loss.[33]

DISCUSSION

Our work integrates detailed molecular characterizations from a number of sources, combining knowledge of mutations and other genetic alterations with analysis of gene and protein expression in lung adenocarcinomas. This gives the most comprehensive analysis to date of the consequences of *LKB1* loss in lung adenocarcinomas, and the novel biological insights that we have uncovered will guide future experimentation and may suggest therapeutic strategies to target these tumors. In particular, we show that *LKB1* loss in lung adenocarcinomas is associated with a characteristic pattern of gene expression changes, which can be used to accurately predict *LKB1* loss and is also directly responsive to *LKB1* activation in vitro. We integrate analysis of these gene expression patterns with data on somatic mutations and protein expression to describe novel associations between *LKB1* and other oncogenic pathways, especially activation of the NRF2 pathway for reactive oxygen detoxification and dysregulation of the PI3K/AKT/FOXO3 pathway, both of which have important effects on multiple cellular phenotypes and can affect response to a variety of anticancer treatments. The identification of previously unknown phenotypes associated with *LKB1* loss has also been a major rationale for the development and study of the murine model of *Lkb1/Kras*-mutant lung cancer. However, our meta-analysis of *LKB1*-associated gene expression shows that *LKB1* loss produces distinctly different effects in murine tumors than in human lung adenocarcinomas and cell lines. It is unclear whether the dissimilarity in gene expression reflects differences in clinically relevant phenotypes. Further experimentation is warranted to explore these differences.

Our characterization of gene expression patterns allowed us to develop and validate a 16-gene *LKB1*-loss signature that sensitively detects 93% of *LKB1* mutations in resected lung adenocarcinoma while also identifying tumors that have lost *LKB1* by other mechanisms. Previous analysis of cell lines has shown that homozygous deletion and intragenic deletion are common mechanisms of *LKB1* loss in addition to somatic mutation.[10–12] Our work suggests that sequencing efforts to detect *LKB1* mutations may fail to detect about half the instances of *LKB1* loss. Thus, combination of direct sequencing with an expression-based classifier could enhance detection of *LKB1* loss, for instance to assess the effect of *LKB1* loss on response to mTOR inhibitors or other novel targeted agents in clinical trials.

In addition to the potential use of our signature as a clinical classifier, our study of the dysregulated genes associated with *LKB1* loss has given insight into the biology of *LKB1*-deficient tumors. Other integrated molecular analyses have been applied to lung cancer (Cancer Genome Atlas Research Network. Comprehensive molecular characterization of lung adenocarcinoma. *Nature.* 2014)[18,37,38] and have disclosed novel associations that would be difficult to appreciate with more targeted approaches, including association of *LKB1* mutations with gene expression–defined subtypes of lung adenocarcinoma. Rather than taking a global approach used in many of these studies, our work focused specifically on *LKB1* loss as a single phenotype of interest. Our subsequent analysis confirmed a role of CREB activation that has previously been shown to have important oncogenic effects in *LKB1*-deficient tumors and results from a well-understood mechanism involving *LKB1*-mediated regulation of CRTC transcriptional coactivators.[26–28] Moreover, we identify additional transcription factors FOXO3, FOXA2, and NRF2 that

are active in *LKB1*-deficient tumors and may influence various phenotypes within these tumors. Our in vitro experiments also showed that restoring *LKB1* expression led to down-regulation of significant subsets of these genes, demonstrating that *LKB1* affects the activity of the corresponding transcription factors through direct downstream mechanisms.

Each of the factors we identify is known to influence key phenotypes in cancer. Further studies examining their effects and interactions in the context of *LKB1* loss may be particularly informative. For instance, NRF2 is a key activator of the oxidative stress response and also plays a role in metabolic reprogramming of cancer cells.[39,40] *LKB1*-deficient tumors have been shown to be susceptible to oxidative stress, because they are unable to make the appropriate adaptive responses in metabolism and biosynthesis.[5,41] NRF2 is frequently activated by somatic mutations in *KEAP1* in NSCLC,[42,43] and our analysis of the TCGA lung adenocarcinomas shows that the odds of a tumor having a *KEAP1* mutation are increased more than sixfold among tumors with LKB1 loss. This high level of overlap may suggest that selective pressure exists for the activation of NRF2 as a secondary protective mechanism to compensate for *LKB1* loss.

Down-regulation of the PI3K/AKT pathway is also evident among resected lung adenocarcinomas with *LKB1* loss. The mechanism by which *LKB1* loss decreases PI3K/AKT signaling is unclear, but several possibilities are worth mentioning. One possibility is that mTOR activation resulting from LKB1 loss could result in feedback inhibition of PI3K/AKT signaling,[44] analogous to the effects seen in tumors exhibiting TSC2 loss.[45,46] Direct interaction of LKB1 and AKT has also been demonstrated,[47] and LKB1 has been shown to facilitate AKT activation and exert antiapoptotic effects, including inhibitory phosphorylation of the proapoptotic FOXO3 transcription factor.[47,48] Of note, activation of FOXO3 was also suggested by analysis of gene expression, showing that down-regulation of the PI3K/AKT pathway may result in alterations in downstream pathway activation. This work guides future functional experiments to explore the interplay of *LKB1* with these various pathways and the resulting effects on clinically relevant phenotypes such as response to targeted inhibitors.

ACKNOWLEDGMENTS

The authors thank W. Pao, D. Kaufman, A. Russo, for their critical review of the article, and E. Kaufman, for her support. The authors thank the efforts of The Cancer Genome Atlas for their extensive molecular characterization of lung and other cancers and thank the many donors of tumor material who have made such resources possible.

Supported by the Strategic Partnering to Evaluate Cancer Signatures (SPECS) grant: NCI U01CA114771.

REFERENCES

1. Ji H, Ramsey MR, Hayes DN, et al. LKB1 modulates lung cancer differentiation and metastasis. *Nature* 2007;448:807–810.
2. Sanchez-Cespedes M, Parrella P, Esteller M, et al. Inactivation of LKB1/STK11 is a common event in adenocarcinomas of the lung. *Cancer Res* 2002;62:3659–3662.
3. Shaw RJ, Bardeesy N, Manning BD, et al. The LKB1 tumor suppressor negatively regulates mTOR signaling. *Cancer Cell* 2004;6:91–99.
4. Carretero J, Medina PP, Blanco R, et al. Dysfunctional AMPK activity, signalling through mTOR and survival in response to energetic stress in LKB1-deficient lung cancer. *Oncogene* 2007;26:1616–1625.
5. Shackelford DB, Abt E, Gerken L, et al. LKB1 inactivation dictates therapeutic response of non-small cell lung cancer to the metabolism drug phenformin. *Cancer Cell* 2013;23:143–158.
6. Shackelford DB, Shaw RJ. The LKB1-AMPK pathway: metabolism and growth control in tumour suppression. *Nat Rev Cancer* 2009;9:563–575.
7. Alessi DR, Sakamoto K, Bayascas JR. LKB1-dependent signaling pathways. *Annu Rev Biochem* 2006;75:137–163.
8. Carretero J, Shimamura T, Rikova K, et al. Integrative genomic and proteomic analyses identify targets for Lkb1-deficient metastatic lung tumors. *Cancer Cell* 2010;17:547–559.
9. Chen Z, Cheng K, Walton Z, et al. A murine lung cancer co-clinical trial identifies genetic modifiers of therapeutic response. *Nature* 2012;483:613–617.
10. Matsumoto S, Iwakawa R, Takahashi K, et al. Prevalence and specificity of LKB1 genetic alterations in lung cancers. *Oncogene* 2007;26:5911–5918.
11. Gill RK, Yang SH, Meerzaman D, et al. Frequent homozygous deletion of the LKB1/STK11 gene in non-small cell lung cancer. *Oncogene* 2011;30:3784–3791.
12. Esteller M, Avizienyte E, Corn PG, et al. Epigenetic inactivation of LKB1 in primary tumors associated with the Peutz-Jeghers syndrome. *Oncogene* 2000;19:164–168.
13. Liberzon A, Subramanian A, Pinchback R, Thorvaldsdóttir H, Tamayo P, Mesirov JP. Molecular signatures database (MSigDB) 3.0. *Bioinformatics* 2011;27:1739–1740.
14. Subramanian A, Tamayo P, Mootha VK, et al. Gene set enrichment analysis: a knowledge-based approach for interpreting genome-wide expression profiles. *Proc Natl Acad Sci U S A* 2005;102:15545–15550.
15. Lamb J, Crawford ED, Peck D, et al. The Connectivity Map: using gene-expression signatures to connect small molecules, genes, and disease. *Science* 2006;313:1929–1935.
16. Ding L, Getz G, Wheeler DA, et al. Somatic mutations affect key pathways in lung adenocarcinoma. *Nature* 2008;455:1069–1075.
17. Chitale D, Gong Y, Taylor BS, et al. An integrated genomic analysis of lung cancer reveals loss of DUSP4 in EGFR-mutant tumors. *Oncogene* 2009;28:2773–2783.
18. Wilkerson MD, Yin X, Walter V, et al. Differential pathogenesis of lung adenocarcinoma subtypes involving sequence mutations, copy number, chromosomal instability, and methylation. *PLoS One* 2012;7:e36530.
19. Selamat SA, Chung BS, Girard L, et al. Genome-scale analysis of DNA methylation in lung adenocarcinoma and integration with mRNA expression. *Genome Res* 2012;22:1197–1211.
20. Shedden K, Taylor JMG, Enkemann SA, et al. Gene expression–based survival prediction in lung adenocarcinoma: a multi-site, blinded validation study. *Nat Med* 2008;14:822–827.
21. Garnett MJ, Edelman EJ, Heidorn SJ, et al. Systematic identification of genomic markers of drug sensitivity in cancer cells. *Nature* 2012;483:570–575.
22. Barretina J, Caponigro G, Stransky N, et al. The Cancer Cell Line Encyclopedia enables predictive modelling of anticancer drug sensitivity. *Nature* 2012;483:603–607.
23. Hardie DG, Alessi DR. LKB1 and AMPK and the cancer-metabolism link—ten years after. *BMC Biol* 2013;11:36.
24. Kau TR, Schroeder F, Ramaswamy S, et al. A chemical genetic screen identifies inhibitors of regulated nuclear export of a Forkhead transcription factor in PTEN-deficient tumor cells. *Cancer Cell* 2003;4:463–476.
25. Rosenbloom KR, Sloan CA, Malladi VS, et al. ENCODE data in the UCSC Genome Browser: year 5 update. *Nucleic Acids Res* 2013;41(Database issue):D56–D63.
26. Feng Y, Wang Y, Wang Z, et al. The CRTC1-NEDD9 signaling axis mediates lung cancer progression caused by LKB1 loss. *Cancer Res* 2012;72:6502–6511.
27. Screaton RA, Conkright MD, Katoh Y, et al. The CREB coactivator TORC2 functions as a calcium- and cAMP-sensitive coincidence detector. *Cell* 2004;119:61–74.
28. Komiya T, Coxon A, Park Y, et al. Enhanced activity of the CREB co-activator Crtc1 in LKB1 null lung cancer. *Oncogene* 2010;29:1672–1680.
29. Jimenez AI, Fernandez P, Dominguez O, Dopazo A, Sanchez-Cespedes M. Growth and molecular profile of lung cancer cells expressing ectopic

LKB1: down-regulation of the phosphatidylinositol 3'-phosphate kinase/PTEN pathway. *Cancer Res* 2003;63:1382–1388.
30. Lin-Marq N, Borel C, Antonarakis SE. Peutz-Jeghers LKB1 mutants fail to activate GSK-3beta, preventing it from inhibiting Wnt signaling. *Mol Genet Genomics* 2005;273:184–196.
31. Fernandez P, Carretero J, Medina PP, et al. Distinctive gene expression of human lung adenocarcinomas carrying LKB1 mutations. *Oncogene* 2004;23:5084–5091.
32. Kervestin S, Jacobson A. NMD: a multifaceted response to premature translational termination. *Nat Rev Mol Cell Biol* 2012;13:700–712.
33. Koivunen JP, Kim J, Lee J, et al. Mutations in the LKB1 tumour suppressor are frequently detected in tumours from Caucasian but not Asian lung cancer patients. *Br J Cancer* 2008;99:245–252.
34. Laplante M, Sabatini DM. mTOR signaling in growth control and disease. *Cell* 2012;149:274–293.
35. Vivanco I, Sawyers CL. The phosphatidylinositol 3-Kinase AKT pathway in human cancer. *Nat Rev Cancer* 2002;2:489–501.
36. Shaw RJ, Cantley LC. Ras, PI(3)K and mTOR signalling controls tumour cell growth. *Nature* 2006;441:424–430.
37. Cancer Genome Atlas Research Network. Comprehensive genomic characterization of squamous cell lung cancers. *Nature* 2012;489:519–525.
38. Seo JS, Ju YS, Lee WC, et al. The transcriptional landscape and mutational profile of lung adenocarcinoma. *Genome Res* 2012;22:2109–2119.
39. DeNicola GM, Karreth FA, Humpton TJ, et al. Oncogene-induced Nrf2 transcription promotes ROS detoxification and tumorigenesis. *Nature* 2011;475:106–109.
40. Mitsuishi Y, Taguchi K, Kawatani Y, et al. Nrf2 redirects glucose and glutamine into anabolic pathways in metabolic reprogramming. *Cancer Cell* 2012;22:66–79.
41. Jeon SM, Chandel NS, Hay N. AMPK regulates NADPH homeostasis to promote tumour cell survival during energy stress. *Nature* 2012;485:661–665.
42. Singh A, Misra V, Thimmulappa RK, et al. Dysfunctional KEAP1-NRF2 interaction in non-small-cell lung cancer. *PLoS Med* 2006;3:e420.
43. Solis LM, Behrens C, Dong W, et al. Nrf2 and Keap1 abnormalities in non-small cell lung carcinoma and association with clinicopathologic features. *Clin Cancer Res* 2010;16:3743–3753.
44. Rodrik-Outmezguine VS, Chandarlapaty S, Pagano NC, et al. mTOR kinase inhibition causes feedback-dependent biphasic regulation of AKT signaling. *Cancer Discov* 2011;1:248–259.
45. Manning BD, Logsdon MN, Lipovsky AI, Abbott D, Kwiatkowski DJ, Cantley LC. Feedback inhibition of Akt signaling limits the growth of tumors lacking Tsc2. *Genes Dev* 2005;19:1773–1778.
46. Gan B, Lim C, Chu G, et al. FoxOs enforce a progression checkpoint to constrain mTORC1-activated renal tumorigenesis. *Cancer Cell* 2010;18:472–484.
47. Martínez-López N, Varela-Rey M, Fernández-Ramos D, et al. Activation of LKB1-Akt pathway independent of phosphoinositide 3-kinase plays a critical role in the proliferation of hepatocellular carcinoma from nonalcoholic steatohepatitis. *Hepatology* 2010;52:1621–1631.
48. Zhong D, Liu X, Khuri FR, Sun SY, Vertino PM, Zhou W. LKB1 is necessary for Akt-mediated phosphorylation of proapoptotic proteins. *Cancer Res* 2008;68:7270–7277.